Supporting Information

Mixed-valent manganese oxide for catalytic oxidation of Orange II by activation of persulfate: Heterojunction dependence and mechanism

Daoqing Liu, *[a] Qianwei Li,[b] Jinbao Hou,[c] Huazhang Zhao *[a]

[a] Key Laboratory of Water and Sediment Sciences (Ministry of Education), College of Environmental Sciences and Engineering, Peking University, Beijing 100871, People's Republic of China

[b] State Key Laboratory of Heavy Oil Processing, Beijing Key Laboratory of Oil and Gas Pollution Control, China University of Petroleum-Beijing, 18 Fuxue Road, Changping District, Beijing 102249, China

[c] College of Chemical Engineering, Beijing University of Chemical Technology, Beijing 100029, China

* Corresponding author.

Tel/fax: +86-10-62758748; email address: liudaoqing@yeah.net, zhaohuazhang@pku.edu.cn

Experimental Methods

1. Characterization of catalysts

The crystal structure of the materials was identified by X-ray diffraction (XRD) measurement using a Bruker D8 diffractometer (Cu Kα radiation, λ= 0.15406 nm, Bruker-AXS, Karlsruhe, Germany). Fourier transform infrared (FTIR) was obtained in the range of 400-4000 cm^{-1} using a spectrophotometer with KBr as the reference transmittance (IR Affinity-1, Japan). The surface morphology, structure and crystalline phase of materials were observed on a Scanning Electron Microscopy (SEM) and a Transmission Electron Microscope TEM images were recorded with a SU8220 (HITACHI, Japan) and JEM-2100F (JEOL, Japan). The X-ray photoelectron spectroscopy (XPS) measurements were recorded via an XPS spectrometer (EscaLab 250Xi, Thermofisher Scientific Company) with Al Kα monochromator, where all the peak energies were calibrated based on C1 s peak at 284.8eV of external carbon, and the XPS spectra were analysed and fitted using CasaXPS software (version 2.2.27). The pore structure characteristics of the samples were measured with an Autosorb-iQ (Quantachrome, USA), and the SSA values were obtained by Density Functional Theory (DFT) analyses of the isotherms. Aqueous concentrations of manganese were analyzed on an inductively coupled plasma-optical emission spectrometer (ICP-OES, Prodigy ICP, Teledyne Leeman Labs, USA). Electrochemical measurements were performed with a CHI 660E electrochemical station (Chenhua, Shanghai, China) using a three-electrode system.

2. Identification of reaction intermediates

Reaction intermediates for the degradation of Orange II were identified by gas chromatography–mass spectrometry (GC-MS) (Agilent GC7890B-MS5977), and the organics were separated by a HP-5 column. The GC equipment was operated in a temperature programmed mode with an initial temperature of 40°C held for 1 min, then ramped to 280°C with 10°C min-1 rate held at 280 °C for 10min. Helium (99.999%) was used as the carrier gas at a constant flow rate of 1 mL min−1, and the Electron impact (EI) mass spectra were scanned from 0 to 400 m/z. Total organic carbon (TOC) was determined using a analyzer (Shimadzu, TOC-Vcpn, Japan) for selected samples. In order to analyse the effect of the initial solution pH on the degradation of Orange II, the pH was adjusted using H_2SO_4 (0.5 mol L^{-1}) and NaOH (0.5 mol L^{-1}) after PDS was

added into the solution. For the measurement of TOC, 10 mL sample was taken out at a fixed interval and quenched by 10 mL of 0.3 M sodium nitrite solution and then analysed. Typical quenching tests were carried on mixed-valent MnO_x using tert-butyl alcohol (TBA) and ethanol (EtOH) as quenching agents to identify the dominant reactive radicals for Orange II degradation.

2. Electrochemical measurement

For the electrochemical test, the MnO_2 and mix-valence manganese oxide MnO_x samples were mixed with acetylene black (AB) and polytetrafluoroethylene (PTFE) with a weight ratio of 85:10:5. The samples, AB and PTFE were first mixed together with ethanol, and then rolled into sheets and punched into disks of 1.4 cm in diameter. After dried overnight at 75°C under vacuum, the disks were pressed onto Pt foil collectors as the electrodes. The electrochemical measurements were carried out using a CHI660E electrochemical workstation (Chenhua Instruments Co., Shanghai, China) in a three-electrode system, which used in the mixture of 2g L^{-1} PDS and 0.5 M Na_2SO_4 aqueous as the electrolyte with a platinum wire as the counter electrode and a saturated calomel electrode (SCE) as the reference electrode. Cyclic voltammogram (CV) measurements were conducted at a scan rate of 10 mV s^{-1} within the potential window of 0-0.7 V *vs.* SCE. Electrochemical impedance spectroscopy (EIS) was carried out utilizing a 5mV amplitude AC voltage (frequency range from 10^5 to 0.1 Hz) and acquired at −0.2 V *vs.* SCE.

Supplementary Figures and Tables

1. TG curve of MnO_x-10

To better evaluate the weight loss and the valent-change processes of the catalysts, thermogravimetric (TG) analysis was performed. Figure S1 depicted the TG and derivative thermogravimetry (DTG) curves of the MnO_x-10. The weight loss before 350 °C was ascribed to the removal of physically absorbed water (at 60-120 °C) and chemically bound water (at 120-350 °C). A weight loss of 4.8% at 500-600 °C for MnO_x was observed, which was attributed to the transformation of MnO_2 to Mn_2O_3.[1] Besides, the other weight loss at 650-800 °C resulted from the transformation of Mn_2O_3 into Mn_3O_4。[2] The TG results confirmed mix-valent state of MnO_x samples.

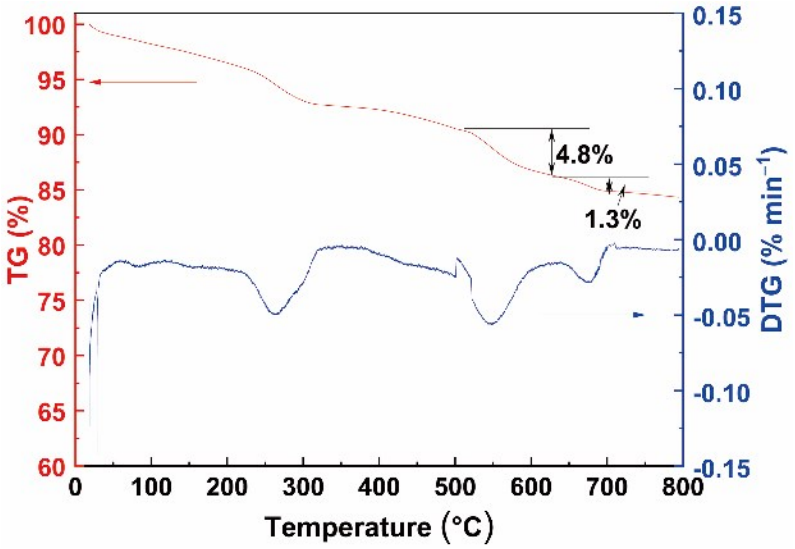

Fig. S1. TG and DTG curves of MnO_x-10 sample

2. Oxidation states analysis of MnO_x by Mn 3s and O 1s

A graphical representation of the separation of peak energies (ΔE) as a function of the manganese oxidation state from the literature data is given in Figure S2.[3] According to the value of ΔE, Figure S2 indicates an average oxidation state of manganese in is in good agreement with that estimated from XPS analysis.

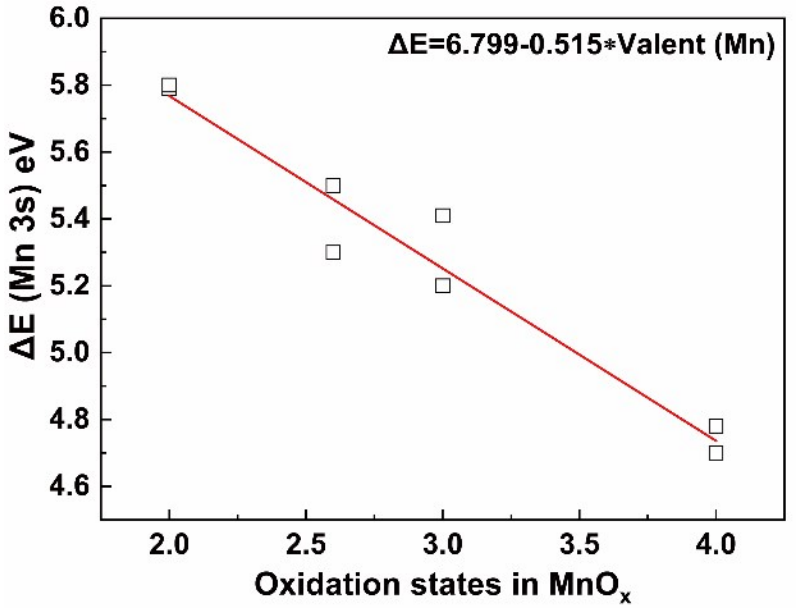

Fig. S2. Separation of peak energies ΔE representative of the Mn 3s multiple splitting as a function of the mean manganese oxidation state

3. Catalytic oxidation of orange II on MnO_x-10

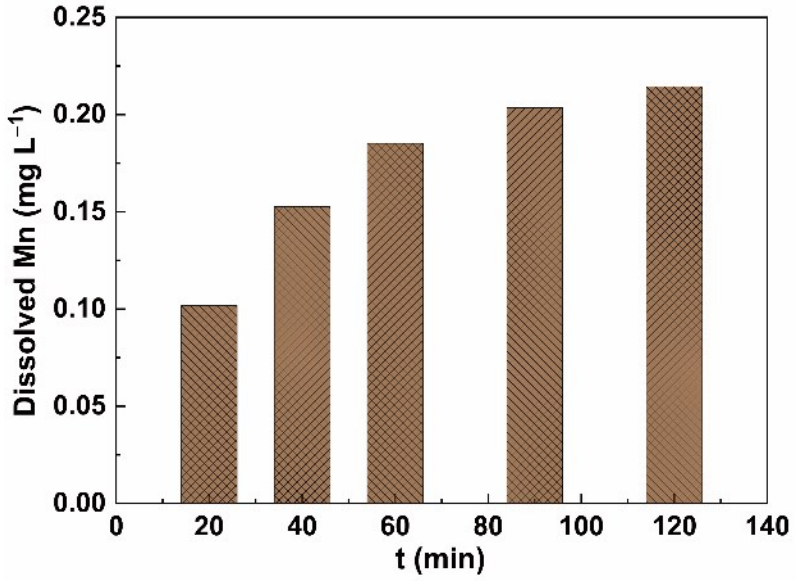

Figure S3. Leaching of Mn ions during Orange Ⅱ degradation

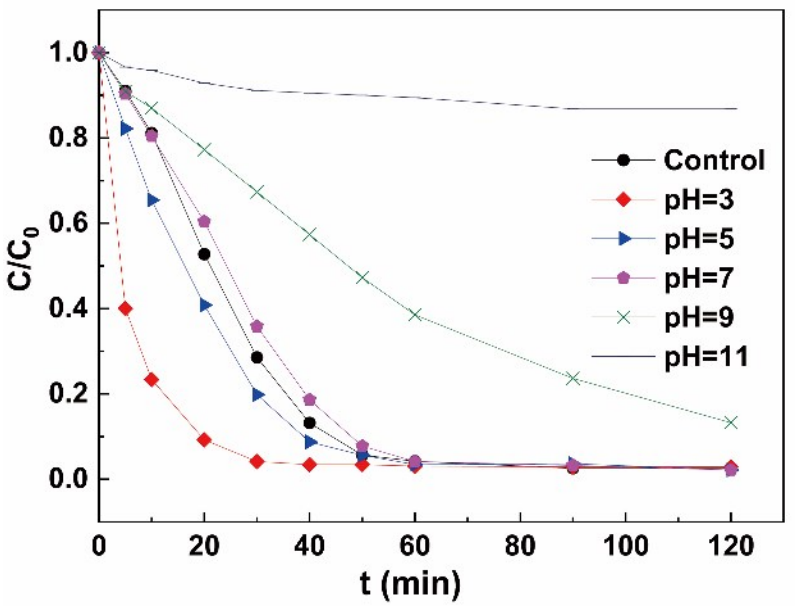

Fig. S4. Effect of solution pH on the Orange II degradation in MnO_x-10/PDS system. (catalyst 0.4 g L^{-1}, PDS 2g L^{-1}, AO II 20 mg L^{-1}, and temperature 25°C.)

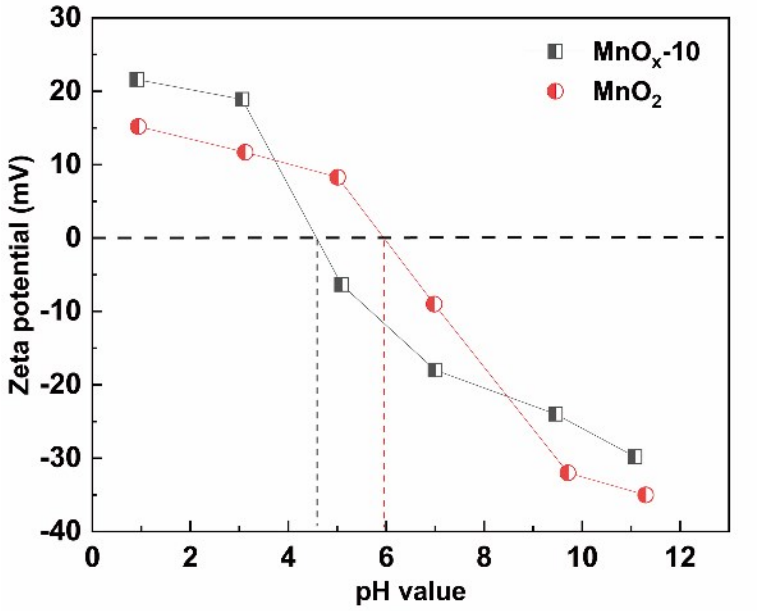

Fig. S5. Zeta potential of MnO_x-10 as a function of pH in aqueous dispersions at a oncentration of 0.5 g ml^{-1}.

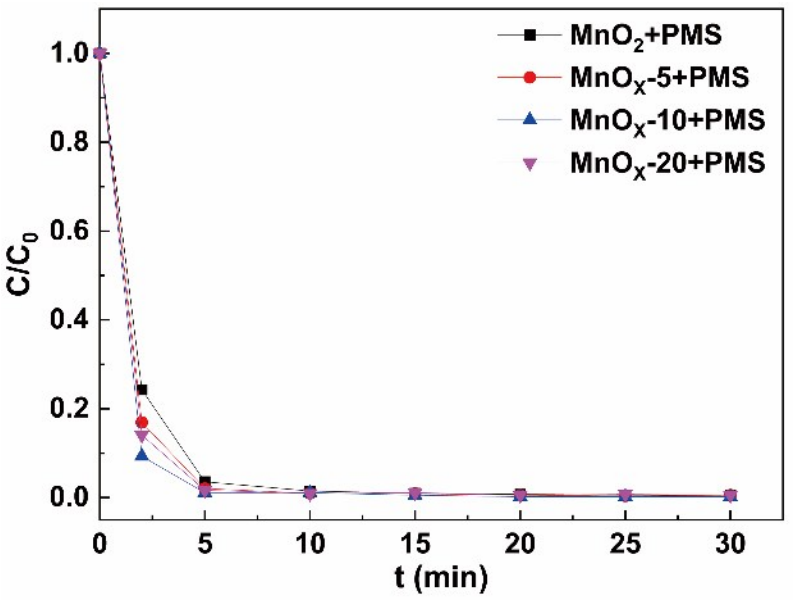

Fig. S6. Orange II removal on manganese oxide catalysts by activation of peroxymonosulfate (PMS). (catalyst 0.4 g L^{-1}, PMS 2g L^{-1}, AO II 20 mg L^{-1}, and temperature 25°C.)

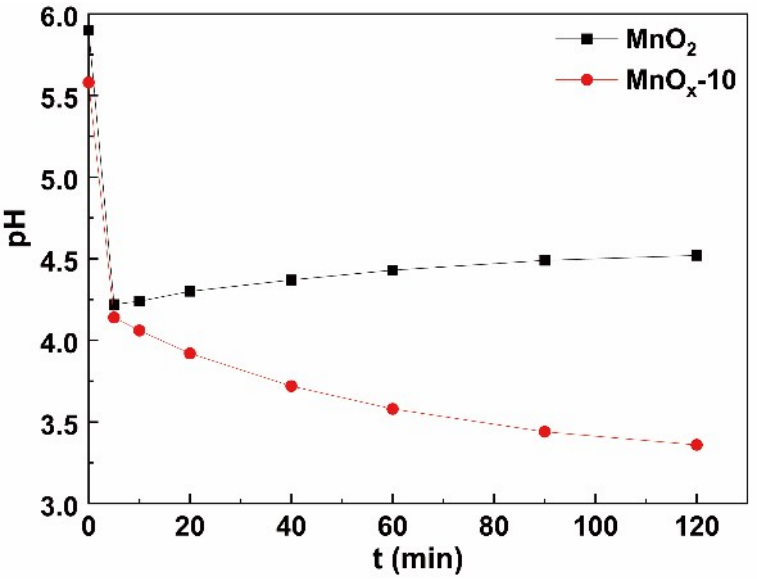

Fig. S7. The pH variations during Orange II degradation procedures by activation of PDS

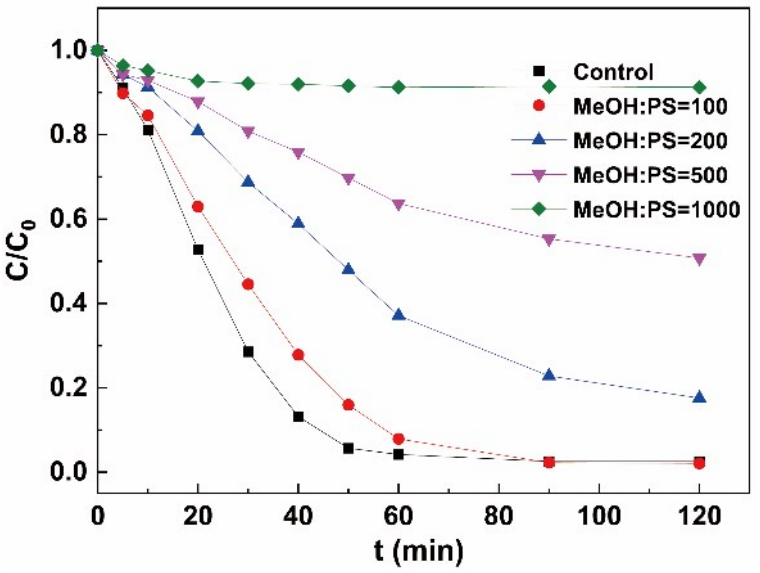

Fig. S8. Effect of methanol quenching on Orange II oxidation on MnO_x-10. (catalyst 0.4 g L^{-1}, PDS 2g L^{-1}, AO II 20 mg L^{-1}, and temperature 25°C.)

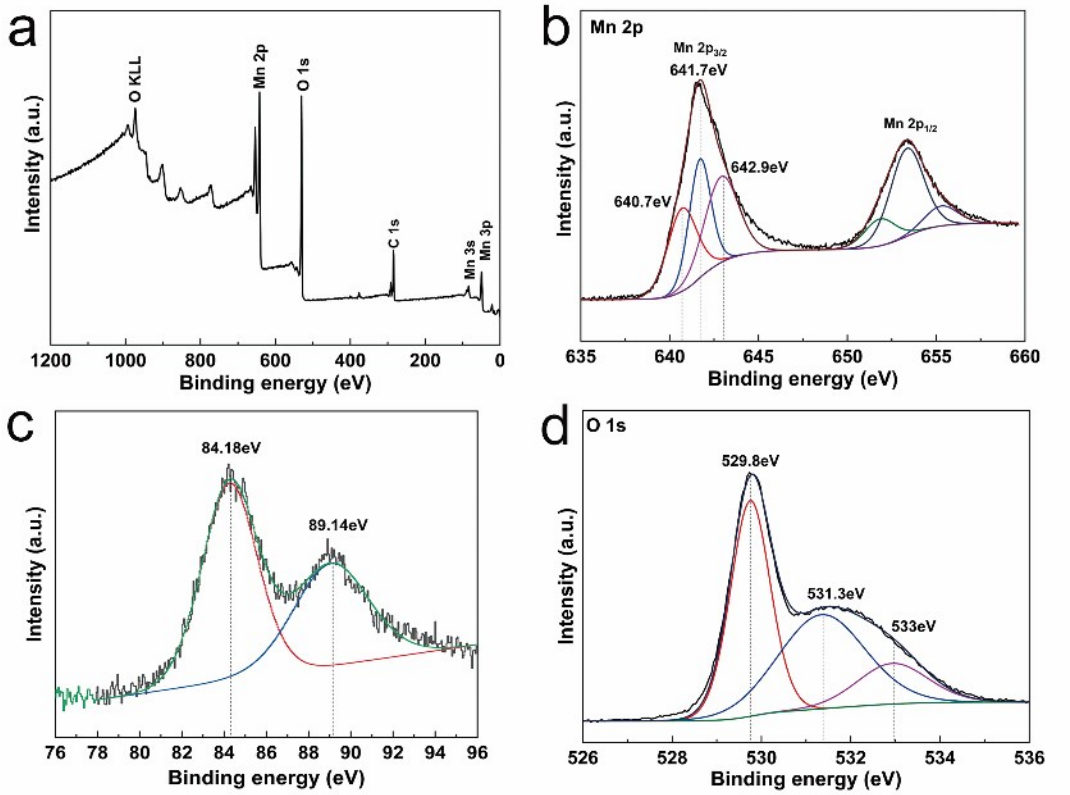

Fig. S9. XPS spectra of MnO_x-10 obtained after reaction.

Table S1. ElS parameters of thin film electrode for MnO_2, MnOx-5, MnOx-10 and MnOx-20.

Sample	Series resistance Rs (Ω)	Charge transfer resistance Rct (Ω)
MnO_2	2.14	32.35
MnO_X-5	2.37	23.73
MnO_X-10	2.65	13.96
MnO_X-20	1.97	19.81

4. GC-MS results

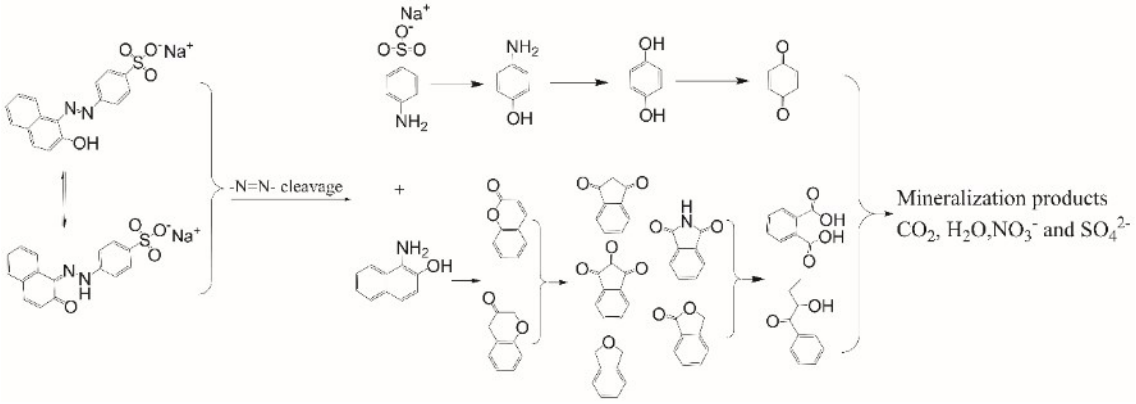

Fig. S10. Proposed degradation pathway of Orange II in the MnO_x-10/PDS system.

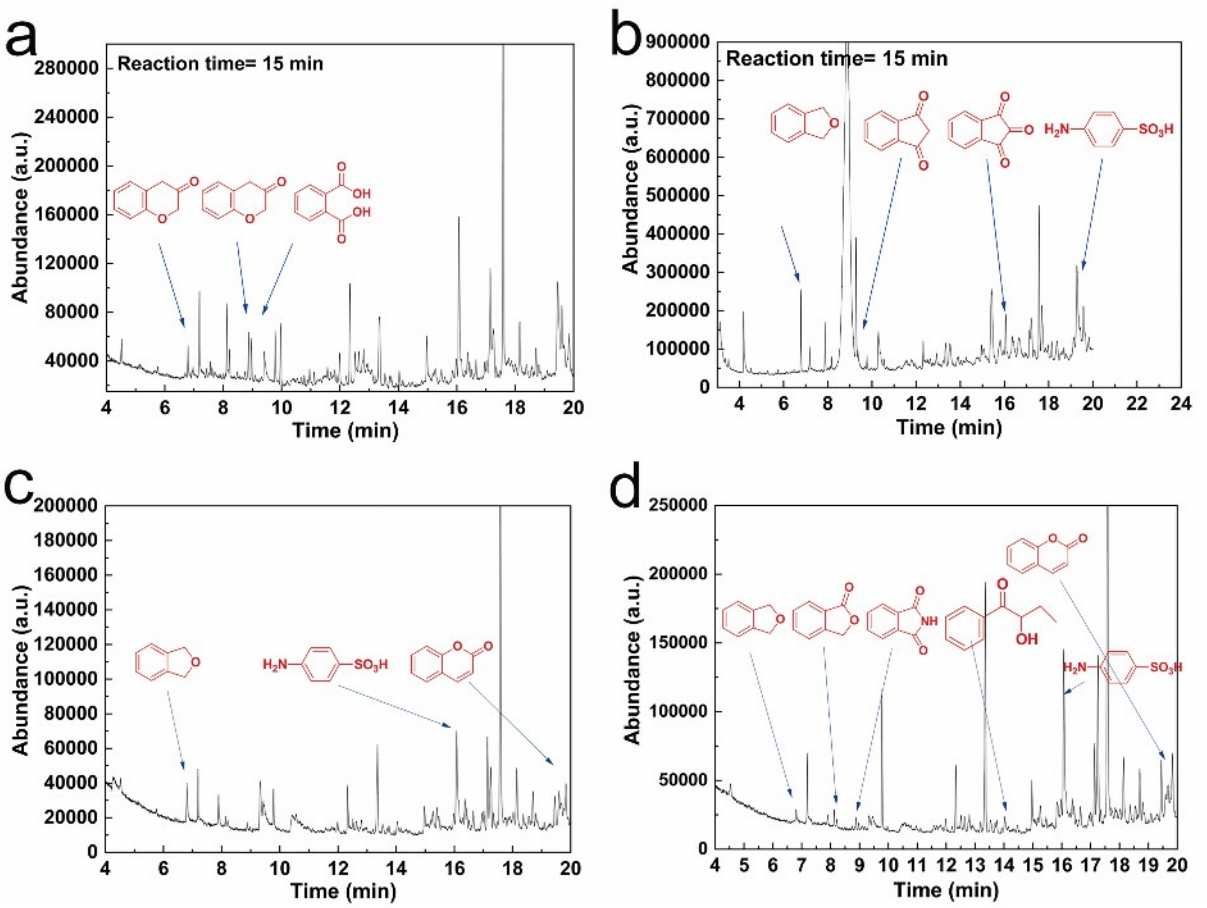

Fig. S11. GC-MS analysis of different reaction time samples

Table S2. Summary of the reaction intermediates detected by GC-MS.

	Retention time (min)	Chemical name	Chemical structure	React time (min)			
				15	30	45	60
A	6.80	1,3-dihydroisobenzofuran	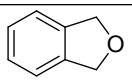	√	√	√	√
B	8.96	chroman-3-one	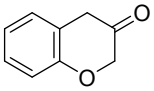	√			
C	9.4	phthalic acid	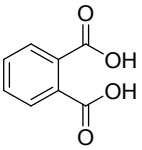	√			
D	8.163	1H-indene-1,3(2H)-dione	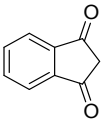		√		
E	13.539	1H-indene-1,2,3-trione	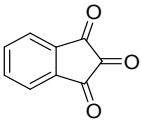		√		
F	16.08	4-aminobenzenesulfonic acid	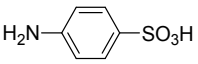		√	√	√
G	19.598	2H-chromen-2-one	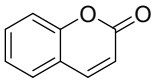			√	√
H	8.216	isobenzofuran-1(3H)-one	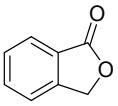				√
J	8.963	isoindoline-1,3-dione	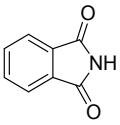				√
K	14.033	2-hydroxy-1-phenylbutan-1-one	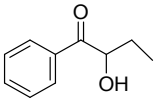				√

5. Catalytic oxidation of orange II on MnO_2 with different nanostructures

The synthesis of MnO_2 with different nanostructures were carried out through a hydrothermal technique similar to that of reported previously.[4] In a typical synthesis of α-MnO_2 nanowires, a 60 mL aqueous solution containing 0.6 g of $MnSO_4 \cdot H_2O$ and 1.5 g of KMnO4 was transferred into a 100 mL Teflon-lined stainless steel autoclave and kept at 140 °C for 12h (MnO_2-12h). The product was filtered, washed with distilled water, and then dried at 80 °C for 6 h in air. Flower-nanowire mixed α-MnO_2 were prepared by altering the dwelling time to 6h (MnO_2-12h). The characterizations and catalytic degradation experiments results are shown as follows.

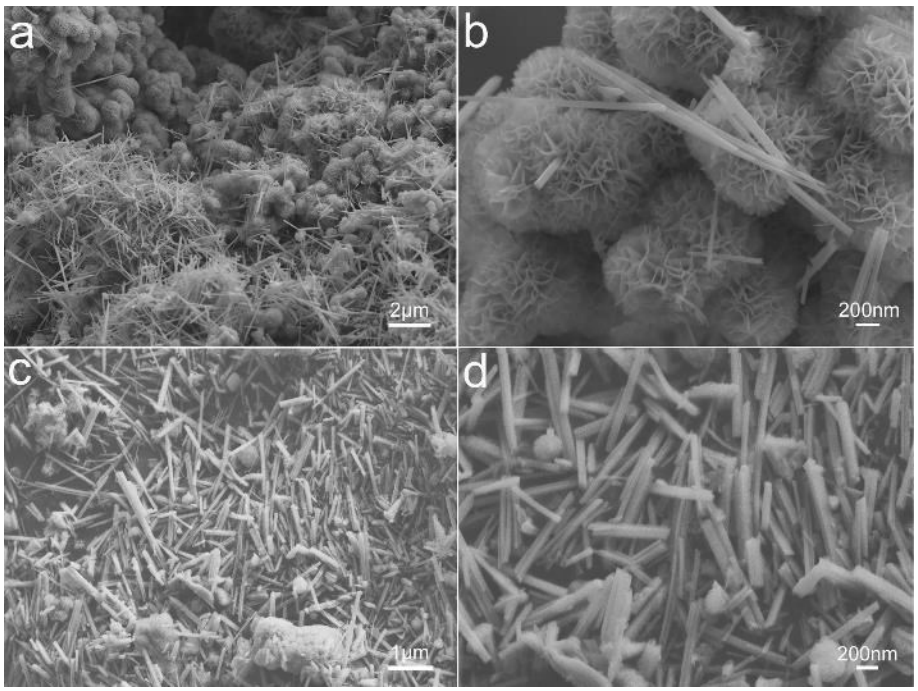

Fig. S12. SEM images of the as-prepared materials: (a and b) Flower-nanowire mixed α-MnO_2 (6 h), (c and d) α-MnO_2 nanowires (12h).

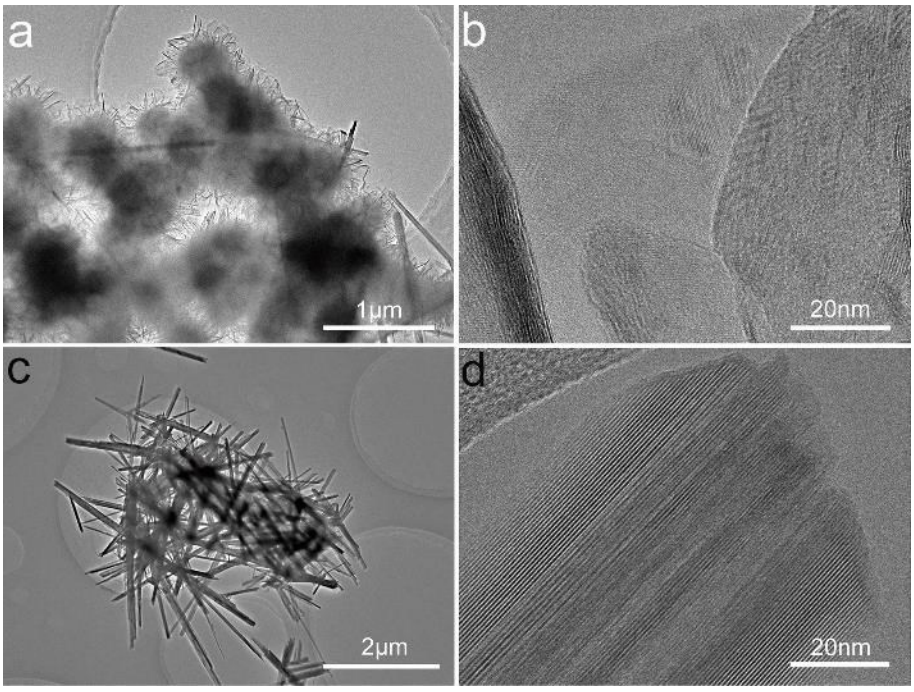

Fig. S13. TEM and high resolution TEM images of the as-prepared materials: (a and b) Flower-nanowire mixed α-MnO_2 (MnO_2-6 h), (c and d) α-MnO_2 nanowires (MnO_2-12h).

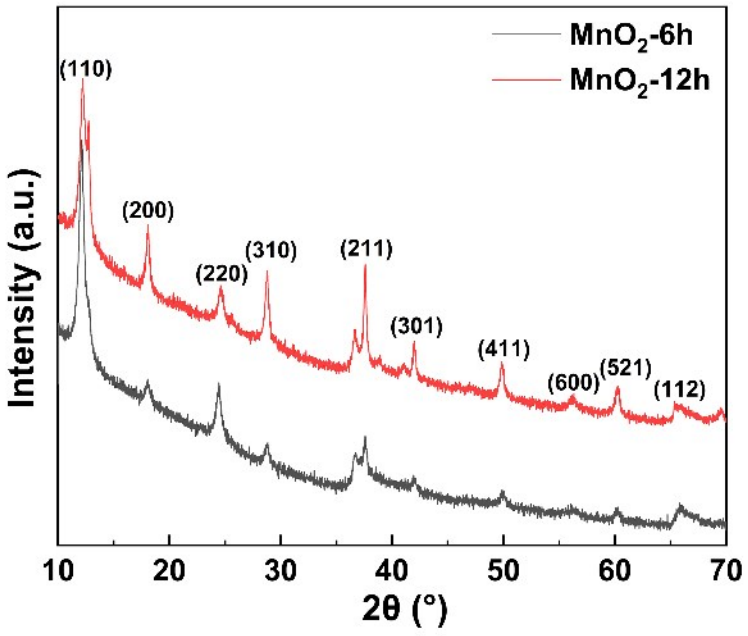

Fig. S14. XRD patterns of MnO_2-6h and MnO_2-12h

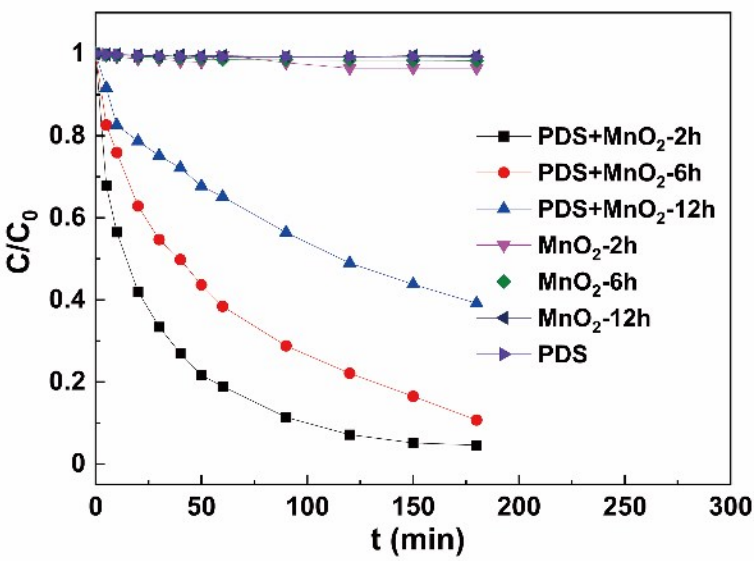

Fig S15. Orange II removal on MnO_2 with different nanostructures; For all reaction conditions: catalyst 0.4 g L^{-1}, PDS 2g L^{-1}, Orange II 20 mg L^{-1}, and temperature 25°C.

6. Catalytic oxidation of orange II on pure MnO_2, Mn_2O_3, Mn_3O_4 and MnOOH

In this part of the research, a manganese dioxide (MnO_2) was purchased from Energy-Chemical Company (China) and used without further treatment. Mn_2O_3 was obtained by treating MnO_2 at 550°C in air for 5h, and Mn_3O_4 was obtained by treating MnO_2 at 950°C in air for 2h according to reported previously.[5]

MnOOH was obtained by ethanol reduction reaction. For a typical synthesis, 3 mL absolute ethanol was added into 47 mL of aqueous solution of $KMnO_4$ (0.1 M) under vigorous stirring at room temperature. The obtained mixture was transferred into Teflon-lined stainless autoclaves and heated at 140 °C for 24 h. The product was filtered, washed with distilled water, and then dried at 80 °C for 6 h in air.[6]

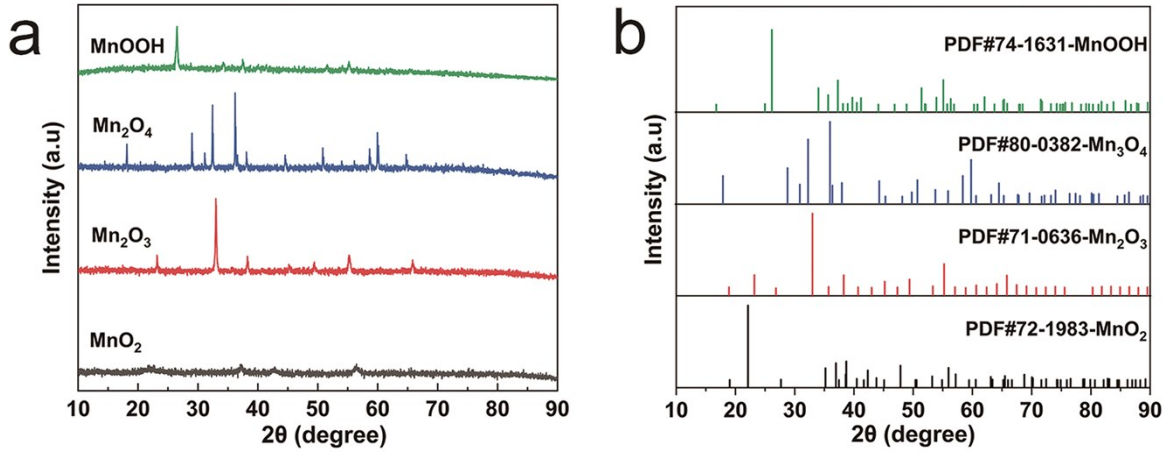

Fig 16. (a) XRD patterns and (b) corresponding pdf card of MnO_2, Mn_2O_3, Mn_3O_4 and MnOOH.

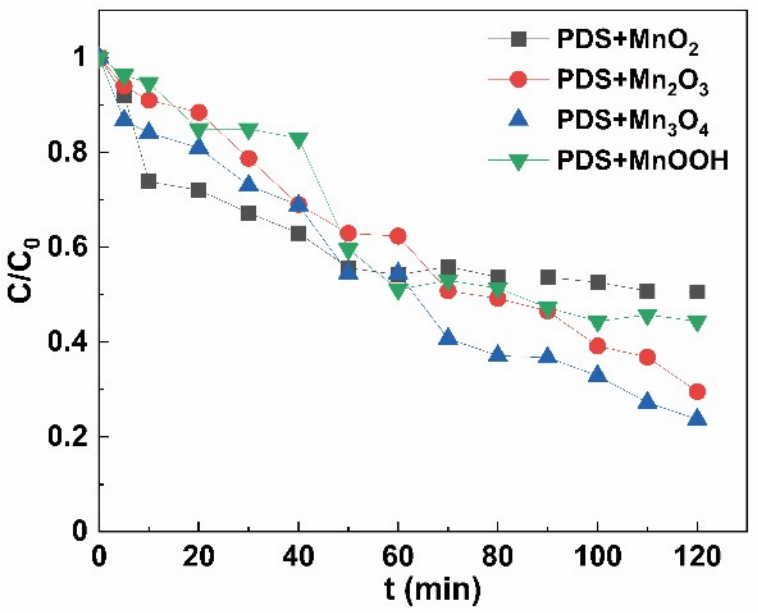

Fig S17. Orange II removal on manganese oxides with pure MnO_2, Mn_2O_3, Mn_3O_4 and MnOOH; For all reaction conditions: catalyst 0.4 g L^{-1}, PDS 2g L^{-1}, Orange II 20 mg L^{-1}, and temperature 25°C.

7. Catalytic oxidation of nitrobenzene and benzoic acid on MnO_x−10

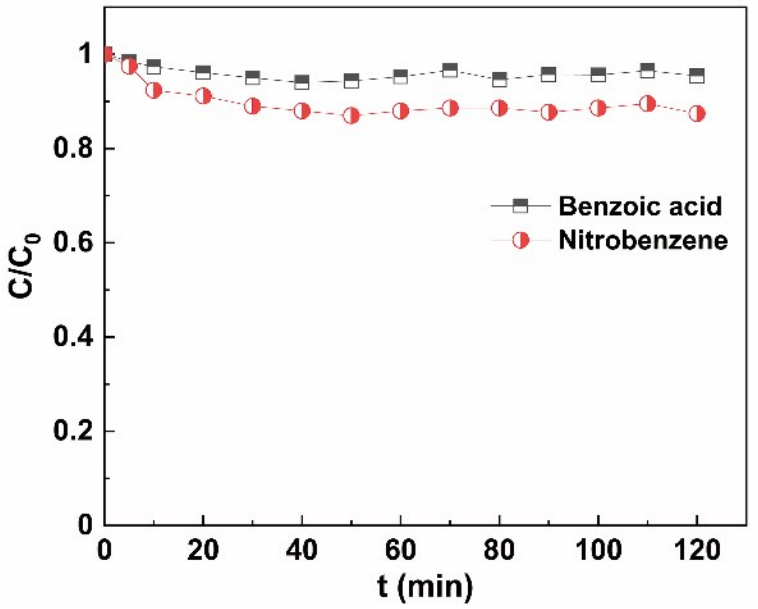

Fig. S18. Catalytic oxidation in MnO_x-10 /PDS activation. For all reaction conditions: catalyst 0.4 g L^{-1}, PDS 2g L^{-1}, organics 100 μM, and temperature 25°C.

8. The quenching effect of singlet oxygen on Orange II oxidative degradation with furfuryl alcohol (FFA)

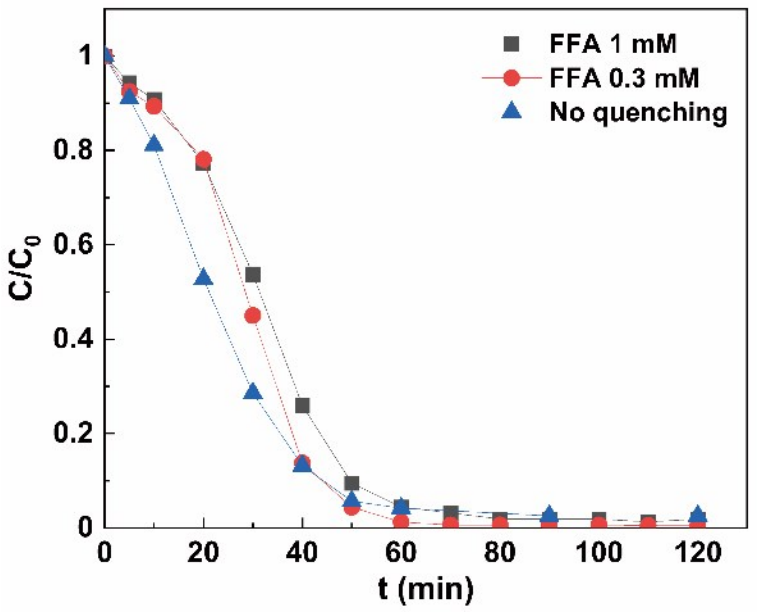

Fig. S19. The quenching effect of singlet oxygen on Orange II oxidative degradation (FFA 0.3−1 mM)

Supplementary References

1. S.-J. Bao, B.-L. He, Y.-Y. Liang, W.-J. Zhou and H.-L. Li, Synthesis and electrochemical characterization of amorphous MnO2 for electrochemical capacitor, *Materials Science and Engineering: A*, 2005, **397**, 305-309.
2. J. Y. Zhu and J. H. He, Facile Synthesis of Graphene-Wrapped Honeycomb MnO2 Nanospheres and Their Application in Supercapacitors, *ACS Appl. Mater. Inter.*, 2012, **4**, 1770-1776.
3. M. Toupin, T. Brousse and D. Belanger, Influence of microstucture on the charge storage properties of chemically synthesized manganese dioxide, *Chem. Mater.*, 2002, **14**, 3946-3952.
4. F. Y. Cheng, Y. Su, J. Liang, Z. L. Tao and J. Chen, MnO2-Based Nanostructures as Catalysts for Electrochemical Oxygen Reduction in Alkaline Media, *Chem. Mater.*, 2010, **22**, 898-905.
5. E. Saputra, S. Muhammad, H. Q. Sun, H. M. Ang, M. O. Tade and S. B. Wang, Manganese oxides at different oxidation states for heterogeneous activation of peroxymonosulfate for phenol degradation in aqueous solutions, *Appl. Catal. B: Environ.*, 2013, **142**, 729-735.
6. T. Gao, F. Krumeich, R. Nesper, H. Fjellvag and P. Norby, Microstructures, Surface Properties, and Topotactic Transitions of Manganite Nanorods, *Inorg. Chem.*, 2009, **48**, 6242-6250.